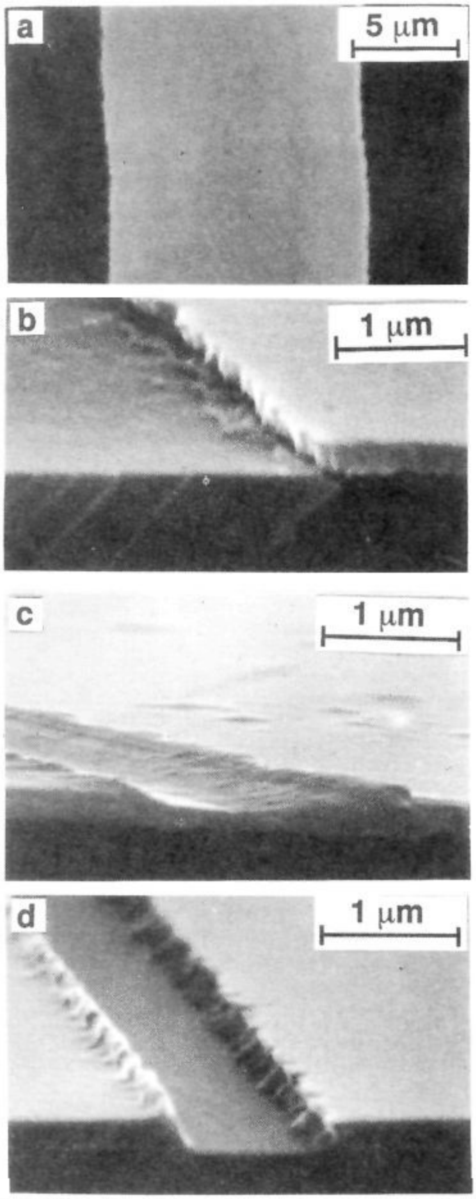

Figure 1. (a) Scanning electron micrograph of a protected Au line (the central stripe; ~12 μm wide) formed by etching. Note the lack of pitting on the protected region. Such protected lines could be extended for centimeters. (b) Profile of a protected line (obtained by fracturing the silicon wafer perpendicular to the line) showing the resolution of the edge after exposure to the CN^-/O_2 etch. (c) Fractured profile of a micromachined trench before etching. (d) Side profile of a trench after etching.

isolated from each other, with resistances between them greater than 1 MΩ.

We were also able to micromachine lines reproducibly in the monolayer, with very high spatial resolution, and subsequently to etch away the gold in the machined regions (Figure 1).[9,10] As with the protected Au line, the edges of the trench exhibited excellent sharpness.

SAMs—14–20 Å, ordered, organic layers[8,11]—can thus protect a surface from corrosion. This thin organic resist material, in combination with patterning and selective etching, provides a convenient method for forming structures of gold on silicon, with feature sizes as small as 1 μm. Because this procedure does not require photolithographic equipment, it is particularly suitable for use in chemical laboratories and for applications such as rapid prototyping of microelectrode arrays and other relatively simple structures.

---

(10) The width of the trench was dependent upon the sharpness of the mechanical probe and the pressure used in the micromachining process. We routinely formed trenches of width 0.5–2 μm. Abbott, N. L.; Folkers, J. P.; Whitesides, G. M. *Science* **1992**, *257*, 1380.

(11) SAMs formed from alkanethiols with longer chains also exhibited excellent protection. Shorter chain thiols including perfluorinated systems provided limited protection from the etching.

Spectroscopic and Theoretical Description of the Electronic Structure of the $S = {}^3/_2$ Nitrosyl Complex of Non-Heme Iron Enzymes

Yan Zhang, Mark A. Pavlosky, Carl A. Brown,
Tami E. Westre, Britt Hedman,† Keith O. Hodgson, and
Edward I. Solomon*

Department of Chemistry, Stanford University
Stanford, California 94305-5080
Stanford Synchrotron Radiation Laboratory
Stanford University
Stanford, California 94309-0210

Received June 30, 1992

Non-heme iron centers are present in the catalytic active sites of a large number of enzymes which are involved in the binding and activation of dioxygen.[1] A member of this class, soybean lipoxygenase (SBL), catalyzes the reaction of 1,4-unsaturated lipids with dioxygen to form a hydroperoxide product.[2] Nitrosyl complexes of enzymes serve as reversible analogues of possible dioxygen intermediates involved in catalysis. SBL-NO and other non-heme ferrous enzyme nitrosyl complexes (formulated as $\{FeNO\}^7$)[3] exhibit an unusual $S = {}^3/_2$ EPR signal,[4] which is also observed in $\{FeNO\}^7$ model complexes.[5] A wide range of bonding descriptions have appeared[6] for these complexes, which include $[Fe^+d^7(S = {}^3/_2)\text{-}NO^+(S = 0)]$, $[Fe^{2+}d^6(S = 2)\text{-}NO^0(S = {}^1/_2)]$ antiferromagnetically coupled, $[Fe^{3+}d^5(S = {}^1/_2)\text{-}NO^-(S = 1)]$ ferromagnetically coupled, and $[Fe^{3+}d^5(S = {}^3/_2)\text{-}NO^-(S = 0)]$. In order for the NO derivative of these enzymes to be used as a probe of electron distribution related to dioxygen reactivity, a clear understanding of the electronic structure and associated spectral features of the $S = {}^3/_2$ $\{FeNO\}^7$ unit is required. Spectroscopic techniques and theoretical methods have been used to study SBL-NO and two $S = {}^3/_2$ ground-state model complexes,[7] $FeL(NO)(N_3)_2$, where L = *N*,*N'*,*N''*-trimethyl-1,4,7-triazacyclononane and FeEDTA-NO. These studies have produced a new bonding

---

* Address correspondence to this author at the Department of Chemistry.

† Stanford Synchrotron Radiation Laboratory.

(1) Solomon, E. I.; Zhang, Y. *Acc. Chem. Res.* **1992**, *25*, 343.

(2) Slappendel, S.; Veldink, G. A.; Vliegenthart, J. F. G.; Aasa, R.; Malmström, B. G. *Biochim. Biophys. Acta* **1983**, *747*, 32.

(3) (a) The Enemark–Feltham[3b] formalism for $\{MNO\}^x$ complexes is used here, in which x is the number of d-type electrons in the system when the nitrosyl ligand is formally considered as NO^+. (b) Enemark, J. H.; Feltham, R. D. *Coord. Chem. Rev.* **1974**, *13*, 339.

(4) (a) Nelson, M. J. *J. Biol. Chem.* **1987**, *262*, 12137. (b) Rich, P. R.; Salerno, J. C.; Leigh, J. S.; Bonner, W. D. *FEBS Lett.* **1978**, *93*, 323. (c) Arciero, D. M.; Lipscomb, J. D. *J. Biol. Chem.* **1986**, *261*, 2170. (d) Arciero, D. M.; Orville, A. M.; Lipscomb, J. D. *J. Biol. Chem.* **1985**, *260*, 14035. (e) Twilfer, H.; Bernhardt, F.-H.; Gersonde, K. *Eur. J. Biochem.* **1985**, *147*, 171. (f) Chen, V. I.; Orville, A. M.; Harpel, M. R.; Frolik, C. A.; Surerus, K. K.; Münch, E.; Lipscomb, J. D. *J. Biol. Chem.* **1989**, *264*, 21677.

(5) Bonner, W. D.; Blum, H.; Rich, P. R.; Salerno, J. C. In *Frontiers of Biological Energetics*; Academic Press: New York, 1978; Vol. II, p 997.

(6) (a) Bill, E.; Bernhardt, F.-H.; Trautwein, A. X.; Winkler, H. *Eur. J. Biochem.* **1985**, *147*, 171. (b) Wells, F. V.; McCann, S. W.; Wickman, H. H.; Kessel, S. L.; Hendrickson, D. N.; Feltham, R. D. *Inorg. Chem.* **1982**, *21*, 2306. (c) Earnshaw, A.; King, E. A.; Larkworthy, L. F. *J. Chem. Soc. A* 1969, 2459. (d) Salerno, J. C.; Siedow, J. N. *Biochem. Biophys. Acta* **1979**, *579*, 246. (e) Pohl, K.; Wieghardt, K.; Nuber, B.; Weiss, J. *J. Chem. Soc., Dalton Trans.* 1987, 187.

(7) Both model systems exhibit $S = {}^3/_2$ EPR spectra and have $\mu_{\text{effective}}$ values of 3.66 and 4.06 at 260 K, respectively, with no spin crossover observed in the temperature range of 2–260 K.

0002-7863/92/1514-9189$03.00/0

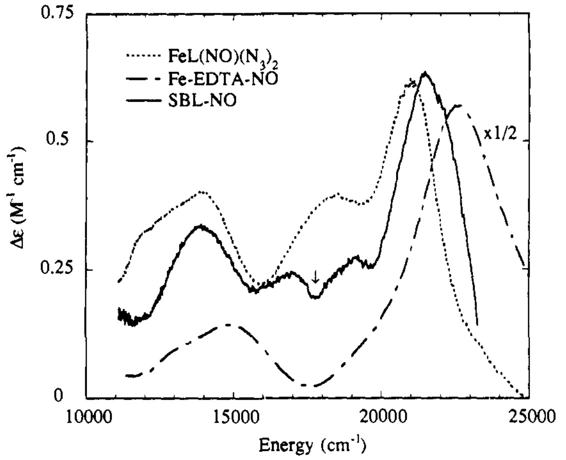

Figure 1. Low-temperature MCD spectra (4.2 K, 5 T) of Fe-SBL-NO (—) (pH 7.6 HEPES buffer, 50% (v/v) glycerol), FeEDTA-NO glass (-·-), and $FeL(NO)(N_3)_2$ mull (···). The ↓ marks a feature due to <1% heme impurity.

description of the $S = {}^3/_2$ $\{FeNO\}^7$ unit involving high-spin Fe^{3+}($S = {}^5/_2$), which is antiferromagnetically coupled to NO^-($S = 1$) through direct orbital overlap.

SBL was purified[8] to a specific activity of >200 units/mg, and the deoxygenated ferrous enzyme was incubated with 1 atm of NO for ~20 min.[9] $FeL(NO)(N_3)_2$ and FeEDTA-NO were prepared according to published procedures.[4d,6e] Magnetic circular dichroism (MCD) spectroscopy,[10] resonance Raman (RR) spectroscopy,[11] normal coordinate analyses,[12] spin-unrestricted SCF-Xα-SW calculation,[13] and X-ray absorption edge spectra (XAS)[14] were performed as described in the associated references.

MCD directly probes the excited states of a complex, providing detailed electronic structural insight. The MCD spectrum of SBL-NO is very similar to those of the two model complexes (Figure 1), with relatively intense transitions in the 22 000 cm^{-1} region and weaker bands to lower energy. Variable-temperature, variable-field MCD data has shown that all of these transitions correlate with the $S = {}^3/_2$ ground state with very similar zero field splittings.[15] These similarities show that the nitrosyl complex of SBL has an electronic structure which parallels that of the $\{FeNO\}^7$ model systems. Therefore, studies on the model complexes can be used to probe the nitrosyl complexes of the non-heme ferrous enzymes.

XAS spectra probe the oxidation state of Fe in these $\{FeNO\}^7$ systems. FeEDTA-NO and Fe^{3+}EDTA exhibit a single 1s → 3d pre-edge feature at ~7112 eV (inset Figure 2), while the pre-edge of Fe^{2+}EDTA is split by 2 eV.[16] Since the initial states of these iron systems are of maximum spin multiplicity, two spin-allowed final states can be reached in the ferrous case, ^4F and ^4P, while only one spin-allowed state of maximum spin multiplicity can be reached in the ferric case, ^5D. The lack of splitting in the 1s → 3d pre-edge peak of FeEDTA-NO indicates that the metal ion is in the ferric oxidation state. The edge energy is dependent upon the effective nuclear charge of the absorbing metal ion.[17] The energy of the FeEDTA-NO edge lies between those of the reduced and oxidized iron–EDTA complexes (Figure 2). As differences between the coordination spheres are minimal, the increase in the edge energy in FeEDTA-NO compared to Fe^{2+}EDTA is mainly due to an increase in the oxidation state of the iron. In addition, the FeEDTA-NO spectrum is similar in intensity and shape to the Fe^{3+}EDTA spectrum. Therefore, XAS spectra indicate that the iron in FeEDTA-NO is best described as ferric. The XAS spectrum of $FeL(NO)(N_3)_2$ (not shown) has an unsplit pre-edge feature, indicating that this iron is also in its ferric oxidation state.

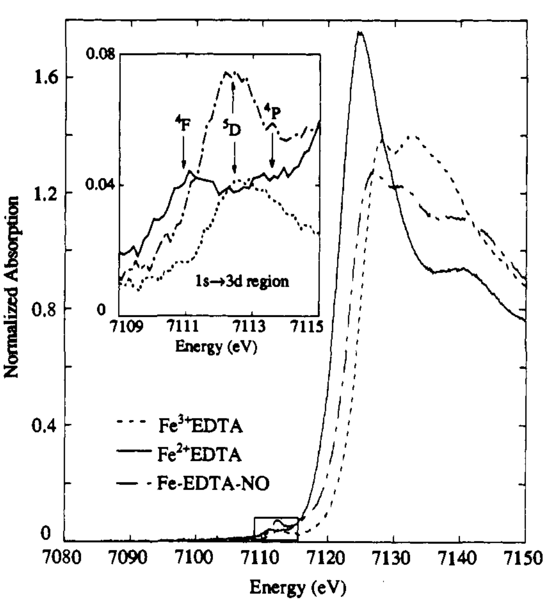

Figure 2. XAS Fe K edge spectra collected on unfocused beamline 7–3 using a Si(220) double crystal monochromator at SSRL. Samples (50 mM) were run at 85 K in fluorescence mode using an Ar-filled ionization chamber equipped with Soller slits and a Mn filter using an internal Fe foil calibrant and assigning the first inflection point to 7111.2 eV. Edge data were measured to $k = 9.5$ Å^{-1}. Five to nine scans were averaged for each sample. Standard pre-edge background subtraction and spline fitting techniques were used to normalize the data.

Isotopically-shifted FeNO-related vibrations were used in a normal coordinate analysis to obtain the intra-NO stretching force constant,[18] which probes the bonding in the bound NO. RR spectra of the two model complexes contain three vibrations which shift upon ^{18}O and ^{15}N substitution of NO. $FeL(NO)(N_3)_2$ exhibits vibrations at 1712, 436, and 498 cm^{-1}, and FeEDTA-NO shows vibrations at 1776, 517, and 496 cm^{-1}, which are assigned as ν(NO), ν(FeN), and δ(FeNO), respectively, on the basis of observed isotopic shifts. Normal coordinate calculations give f(NO) values of 12.6 and 13.4 mdyn/Å for $FeL(NO)(N_3)_2$ and FeEDTA-NO, respectively. Comparison to f(NO) values of 8.4, 15.5, and 21.3 mdyn/Å calculated for NO^-, NO^0, and NO^+, respectively, indicates a form between NO^- and NO^0. Together the XAS and RR data indicate that the Fe^{2+} has transferred an electron to NO, producing a ferric–NO^- complex which has significant electron delocalization.

Spin-unrestricted Xα calculations, for the $S = {}^3/_2$ spin state, have been performed on $[(NH_3)_3(OH)_2FeNO]$ using the coordinates of $FeL(NO)(N_3)_2$,[19] which has a bent FeNO unit with an angle of 155°. A parallel calculation was performed on a linear FeNO $S = {}^3/_2$ structure which shows no qualitative energy preference of the bent over the linear structure. The Fe spin up

---

(8) Nelson, M. J. *Biochemistry* **1988**, *27*, 4273.

(9) On the basis of the MCD data, at NO pressure of 1 atm the conversion of Fe^{2+}SBL to SBL-NO is approximately 30% for a 1.2 mM sample in 50% glycerol. This incomplete conversion at high NO concentration is consistent with a previous report (ref 4a).

(10) Spira-Solomon, D. J.; Allendorf, M. D.; Solomon, E. I. *J. Am. Chem. Soc.* **1986**, *108*, 5318.

(11) Tuczek, F.; Solomon, E. I. *Inorg. Chem.* **1992**, *31*, 944.

(12) Fuhres, H.; Karthaa, V. B.; Kidd, K. G.; Krueger, P. J.; Mantsch, H. H. Computer Programs for Infrared Spectroscopy, Bulletin No. 15, National Research Council of Canada, 1976.

(13) (a) Slater, J. C. *Adv. Quantum Chem.* **1972**, *6*, 1. (b) Johnson, K. H. *Adv. Quantum Chem.* **1973**, *7*, 143.

(14) DeWitt, J. G.; Bentsen, J. G.; Rosenzweig, A. C.; Hedman, B.; Green, J.; Pilkington, S.; Papaefthymiou, G. C.; Dalton, H.; Hodgson, K. O.; Lippard, S. J. *J. Am. Chem. Soc.* **1991**, *113*, 9219.

(15) Zhang, Y.; Pavlosky, M. A.; Brown, C. A.; Westre, T. E.; Hedman, B.; Hodgson, K. O.; Solomon, E. I. Manuscript in preparation.

(16) Shulman, R. G.; Yafet, Y.; Eisenberger, P.; Blumberg, W. E. *Proc. Natl. Acad. Sci. U.S.A.* **1976**, *73*, 1384.

(17) Cramer, S. P.; Eccles, T. K.; Kutzler, F. W.; Hodgson, K. O. *J. Am. Chem. Soc.* **1976**, *98*, 1287.

(18) (a) Miki, E.; Mitzumachi, K.; Ishimori, T.; Okuno, H. *Bull. Chem. Soc. Jpn.* **1973**, *46*, 3779. (b) Quinby-Hunt, M.; Feltham, R. D. *Inorg. Chem.* **1978**, *17*, 2515.

(19) For simplification, the N_3^- ligands were replaced with OH^- ligands and the geometry idealized to C_S. The calculational parameters for α values and sphere radii were obtained as in Gewirth, A. A.; Cohen, S. L.; Schugar, H. J.; Solomon, E. I. *Inorg. Chem.* **1987**, *26*, 1133.

($\uparrow$) and spin down ($\downarrow$) orbitals undergo a large spin polarization splitting, with five occupied predominantly Fe$\uparrow$ orbitals stabilized and the Fe$\downarrow$ counterparts higher in energy and unoccupied, consistent with high-spin ferric calculations.[20] The NO Π^* orbitals also split with the occupied $\Pi^*\downarrow$ stabilized below the Fe$\downarrow$ orbitals due to their spin pairing with the Fe$\uparrow$ d_{xz},d_{yz} electrons. The $\Pi^*\uparrow$ set is higher in energy and unoccupied. This calculation therefore gives five uncompensated spin up electrons on the Fe (ferric) and two spin down electrons in the NO Π^* orbitals (NO$^-$). These are spin paired due to direct orbital overlap. Thus an experimentally and theoretically consistent electronic structure has been generated for the $\{FeNO\}^7$ $S = {}^3/_2$ system, which can be described as high-spin Fe^{3+}($S = {}^5/_2$) antiferromagnetically coupled to NO$^-$(S = 1) to produce the $S = {}^3/_2$ ground state. This new bonding description provides a general understanding of the interaction of NO with the high-spin ferrous site, and the spectral features can be quantitated to provide insight into differences in bonding and electron distribution which can be related to dioxygen activation by non-heme iron enzymes.

Acknowledgment. This research was supported by grants from the NIH (GM40392, E.I.S.) and NSF (CHE91-21576, K.O.H.). Stanford Synchrotron Radiation Laboratory is supported by the Department of Energy, Office of Basic Energy Science, Division of Chemical Science and Division of Material Science, and in part by the NIH NCRR BRTP Program (RR-01209) and DOE's Office of Health and Environmental Research.

---

[20] (a) Butcher, K. D.; Gebhard, M. S.; Solomon, E. I. *Inorg. Chem.* **1990**, *29*, 2067. (b) Butcher, K. D.; Didziulis, S. V.; Briat, B.; Solomon, E. I. *J. Am. Chem. Soc.* **1990**, *112*, 2230.

Synthesis and X-ray Crystal Structure of 11-Bromo-*endo*-9-chloro-7-ethoxybicyclo[5.3.1]undec-1(11)-ene. A Stable, Highly Strained Anti-Bredt Olefin

Geerlig W. Wijsman, Willem H. de Wolf, and
Friedrich Bickelhaupt*

Scheikundig Laboratorium, Vrije Universiteit
De Boelelaan 1083, NL-1081 HV Amsterdam
The Netherlands

Huub Kooíjman and Anthony L. Spek

Bijvoet Center for Biomolecular Research
Vakgroep Kristal- en Structuurchemie
University of Utrecht, Padualaan 8, NL-3584 CH Utrecht
The Netherlands

Received April 3, 1992

Strained and twisted double bonds[1] have fascinated chemists ever since Bredt formulated his famous rule which "forbids" the existence of bridgehead double bonds in the so-called anti-Bredt olefins;[2] current interest is illustrated by recently described, highly strained and "unlikely" representatives of this class.[3,4] Strain leads to increased reactivity,[5] and therefore experimental structures are very rare;[1] in the bridgehead *trans*-cyclooctene family, only one X-ray crystal structure of an uncomplexed member is known.[3,6,7]

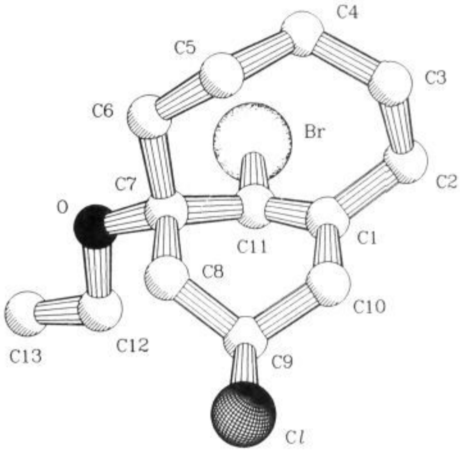

Figure 1. PLUTON drawing of **1** with hydrogen atoms removed for clarity. Selected bond lengths (Å) and bond angles (deg): C1–C2, 1.502 (9); C2–C3, 1.555 (9); C3–C4, 1.541 (8); C4–C5, 1.554 (9); C5–C6, 1.545 (9); C6–C7, 1.554 (9); C7–C11, 1.502 (8); C7–C8, 1.559 (9); C8–C9, 1.520 (8); C9–C10, 1.521 (9); C1–C10, 1.504 (9); C1–C11, 1.319 (8); C2–C1–C10, 117.0 (5); C11–C1–C2, 123.1 (6); C11–C1–C10, 118.6 (5); Br–C11–C7, 112.9 (4); C1–C11–Br, 121.3 (4); C1–C11–C7, 122.9 (5); C1–C2–C3, 105.7 (5); C6–C7–C11, 105.5 (5).

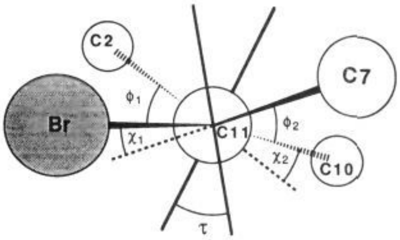

Figure 2. View along the double bond C11═C1. χ_1: 180° – ∠BrC11C1C7 = 20.8 (7)°. χ_2: 180° – ∠C10C1C11C2 = 13.4 (6)°; ϕ_1: ∠BrC11C1C2 = 25.6 (8)°. ϕ_2: ∠C7C11C1C10 = 33.0 (8)°. τ: 0.5(ϕ_1 + ϕ_2) = 29.3°. θ_1: ∠C7C11C1C2 = 133.6 (6)°. θ_2: ∠BrC11C1C10 = 167.8 (4)°.

Scheme I

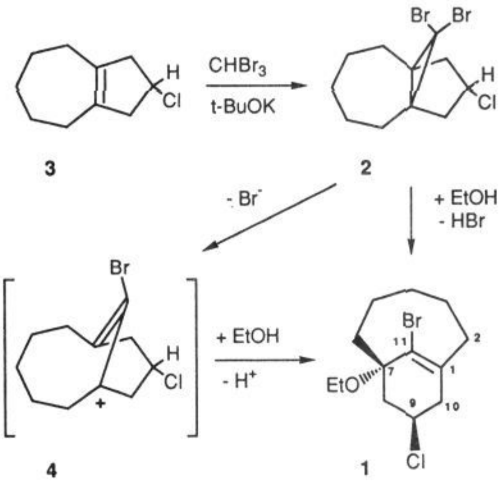

---

[1] Bridgehead olefin reviews: (a) Warner, P. M. *Chem. Rev.* **1989**, *89*, 1067. (b) Keese, R.; Luef, W. *Topics in Stereochemistry*; Eliel, E. L., Wilen, S. H., Eds.; J. Wiley & Sons: New York, 1991; Vol. 20, pp 231–318. (c) Borden, W. T. *Chem. Rev.* **1989**, *89*, 1095. (d) Shea, K. J. *Tetrahedron* **1980**, *36*, 1683. (e) Keese, R. *Angew. Chem.* **1975**, *87*, 568. (f) Buchanan, G. L. *Chem. Soc. Rev.* **1974**, *3*, 41. (g) Buchanan, G. L.; Jamieson, G. *Tetrahedron* **1972**, *28*, 1123. (h) Buchanan, G. L.; Jamieson, G. *Tetrahedron* **1972**, *28*, 1129.

[2] Bredt, J.; Thouet, H.; Schmitz, J. *Justus Liebigs Ann. Chem.* **1924**, *437*, 1.

[3] Shea, K. J.; Lease, T. G.; Ziller, J. W. *J. Am. Chem. Soc.* **1990**, *112*, 8627.

[4] Shimizu, T.; Shimizu, K.; Ando, W. *J. Am. Chem. Soc.* **1991**, *113*, 354.

[5] (a) Warner, P. M.; Peacock, S. *J. Comput. Chem.* **1982**, *3*, 417. (b) Maier, W. F.; von Ragué Schleyer, P. *J. Am. Chem. Soc.* **1981**, *103*, 1891.

[6] For X-ray crystal structures of metal-complexed derivatives, see: (a) Kumar, A.; Lichtenhan, J. D.; Critchlow, S. C.; Eichinger, B. E.; Borden, W. T. *J. Am. Chem. Soc.* **1990**, *112*, 5633. (b) Bly, R. S.; Bly, R. K.; Hossain, M. M.; Lebioda, L.; Raja, M. *J. Am. Chem. Soc.* **1988**, *110*, 7723. (c) Bly, R. S.; Hossain, M. M.; Lebioda, L. *J. Am. Chem. Soc.* **1985**, *107*, 5549. (d) Godleski, S. A.; Gundlach, K. B.; Valpey, R. S. *Organometallics* **1985**, *4*, 296.

0002-7863/92/1514-9191$03.00/0